© 2014. Published by The Company of Biologists Ltd | Development (2014) 141, 399-409 doi:10.1242/dev.094995

RESEARCH ARTICLE

Aberrant cochlear hair cell attachments caused by Nectin-3 deficiency result in hair bundle abnormalities

Terunobu Fukuda[1,2,*], Kanoko Kominami[1,*], Shujie Wang[3], Hideru Togashi[1], Ken-ichi Hirata[2], Akira Mizoguchi[3], Yoshiyuki Rikitake[1,2,4,‡] and Yoshimi Takai[1,5,‡]

ABSTRACT

The organ of Corti consists of sensory hair cells (HCs) interdigitated with nonsensory supporting cells (SCs) to form a checkerboard-like cellular pattern. HCs are equipped with hair bundles on their apical surfaces. We previously reported that cell-adhesive nectins regulate the checkerboard-like cellular patterning of HCs and SCs in the mouse auditory epithelium. Nectin-1 and -3 are differentially expressed in normal HCs and SCs, respectively, and in Nectin-3-deficient mice a number of HCs are aberrantly attached to each other. We show here that these aberrantly attached HCs in Nectin-3-deficient mice, but not unattached ones, show disturbances of the orientation and morphology of the hair bundles and the positioning of the kinocilium, with additional abnormal localisation of cadherin–catenin complexes and the apical-basal polarity proteins Pals1 and Par-3. These results indicate that, owing to the loss of Nectin-3, hair cells contact each other inappropriately and form abnormal junctions, ultimately resulting in abnormal hair bundle orientation and morphology.

KEY WORDS: Cell adhesion, Nectin, Polarity, Mouse

INTRODUCTION

The tissues and organs in mammals are composed of multiple heterogeneous cell types, which are arranged in complex patterns, including the checkerboard-like cell arrangement. In the organ of Corti, the auditory epithelium of the snail-shaped cochlea in the inner ear, sensory hair cells (HCs) are interdigitated with nonsensory supporting cells (SCs), forming a checkerboard-like cellular pattern (Barald and Kelley, 2004; Klein and Mlodzik, 2005) (Fig. 1A-D). In addition to this unique cell arrangement, HCs are equipped with a uniform orientation of hair bundles on their apical surfaces (Fig. 1C,D). This polarised pattern of the hair bundles is a typical example of planar cell polarity (PCP), which refers to the polarisation of a field of cells within the plane of a cell layer. The checkerboard-like cell arrangement and the polarised structures of the hair bundles are essential for appropriate perception of sound (Yoshida and Liberman, 1999).

[1]Division of Molecular and Cellular Biology, Department of Biochemistry and Molecular Biology, Kobe University Graduate School of Medicine, Kobe 650-0017, Japan. [2]Division of Cardiovascular Medicine, Department of Internal Medicine, Kobe University Graduate School of Medicine, Kobe 650-0017, Japan. [3]Department of Neural Regeneration and Cell Communication, Mie University Graduate School of Medicine, Tsu 514-8507, Japan. [4]Division of Signal Transduction, Department of Biochemistry and Molecular Biology, Kobe University Graduate School of Medicine, Kobe 650-0017, Japan. [5]Division of Pathogenetic Signaling, Department of Biochemistry and Molecular Biology, Kobe University Graduate School of Medicine, Kobe 650-0047, Japan.
*These authors contributed equally to this work

‡Authors for correspondence (rikitake@med.kobe-u.ac.jp; ytakai@med.kobe-u.ac.jp)

Received 1 February 2013; Accepted 24 October 2013

The hair bundles on HCs are actin-based structures uniformly aligned on the apices of HCs with V-shapes pointing unidirectionally and abneurally towards the outer (lateral) border of the cochlear duct. In mice, the development and maturation of the hair bundles occur from two perpendicular directions, from the basal to the apical turn and from the medial to the lateral side of the cochlea, during a period between the late embryonic stage and postnatal day (P) 14 (Denman-Johnson and Forge, 1999). During this period, a single tubulin-based kinocilium, a specialised primary cilium extending from the basal body, emerges in the centre of the HC surface (Fig. 1E), and then undergoes directed migration towards the lateral edge. Subsequently, stereocilia become organised around the kinocilium to form the V-shaped bundles (Fig. 1F). The kinocilium retracts at ~P10 (Fig. 1G).

The mechanism underlying the polarity of the kinocilium and stereocilia on HCs (hereafter referred to as HC polarity) is not fully understood, although many PCP molecules have been identified as regulators of HC polarity. These include frizzled (Fz), dishevelled, Celsr, vang-like (Vangl) and prickle (Goodrich and Strutt, 2011; Gray et al., 2011). Ciliary proteins, such as Kif3a and Lis1, also contribute to proper HC polarity with appropriate organisation of microtubules (Sipe et al., 2013; Sipe and Lu, 2011).

The mechanism underlying the checkerboard-like cellular patterning of HCs and SCs had not been revealed, but we recently found that nectins, immunoglobulin-like cell-cell adhesion molecules (CAMs), which comprise a family of four members (Nectin-1, -2, -3 and -4; now known as Pvrl1-4 – Mouse Genome Informatics), regulate this mechanism in the mouse auditory epithelium (Togashi et al., 2011). The characteristic features of nectins are that they promote homophilic and heterophilic *trans*-interactions between members (heterophilic *trans*-interactions are Nectin 1–3, Nectin 1–4 and Nectin 2–3), and that their heterophilic interactions are stronger than their homophilic interactions in the following order: Nectin 1–3>Nectin 2–3>Nectin 1–1, 2–2 and 3–3 (Harrison et al., 2012; Ikeda et al., 2003). In mice, Nectin-1, -2 and -3 are expressed in the auditory epithelium, of which Nectin-1 and -3 are differentially expressed in HCs and SCs, respectively. Genetic deletion of *Nectin-3* leads to disruption of the checkerboard-like cellular pattern with aberrant attachments between HCs by a homophilic interaction of Nectin-1. Thus, the heterophilic *trans*-interaction between Nectin-1 in HCs and Nectin-3 in SCs mediates heterotypic adhesion between these two cell types and contributes to the checkerboard-like cellular patterning.

Nectins are involved in the formation of adherens junctions (AJs) cooperatively with cadherins in various cell types, including epithelial and endothelial cells and fibroblasts (Takai et al., 2008a; Takai et al., 2008b). In addition, nectins regulate the formation of tight junctions (TJs), of which major CAMs are junctional adhesion molecules (JAMs), occludin and claudins, which act cooperatively with cadherins (Takai et al., 2008a; Takai et al., 2008b).

Development (2014) doi:10.1242/dev.094995

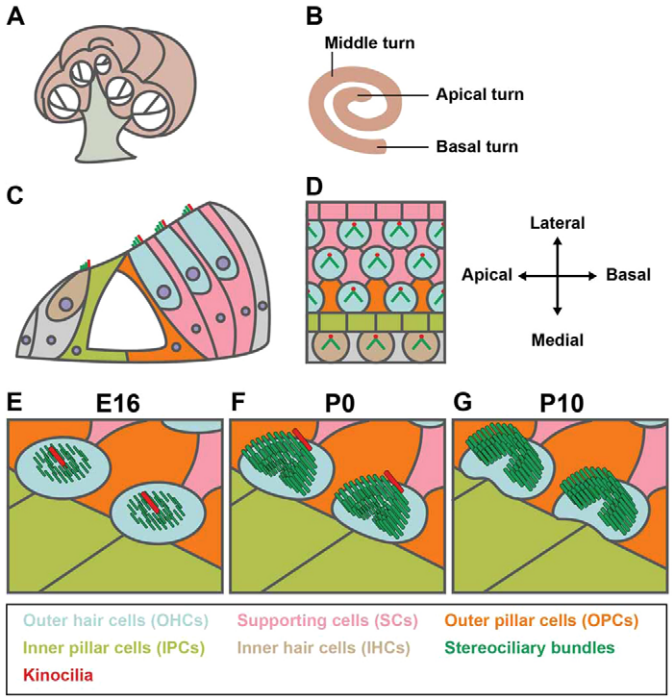

Fig. 1. Auditory epithelium of the cochlea in the inner ear. (A) Entire view of the cochlea. (B) Coiled duct. (C) The organ of Corti. (D) A checkerboard-like cellular pattern. In the auditory epithelium, inner and outer HCs are interdigitated with several types of SCs, including inner phalangeal, inner and outer pillar, and Deiters cells. (E-G) The patterning of the hair bundles in the developing mammalian cochlear duct. The kinocilium emerges from the centre of the apical surface of HCs at E16 (E) and then undergoes directed migration towards the lateral edge, where stereocilia are organised around it to form V-shaped bundles at P0 (F). The kinocilium is finally retraced at around P10 (G). See Togashi et al. (Togashi et al., 2011).

During the course of a study on the roles of nectins in the checkerboard-like cellular patterning of HCs and SCs in the mouse auditory epithelium, we noticed that the hair bundles were morphologically abnormal in Nectin-3-deficient mice compared with those in wild-type mice. Therefore, in the present study, we investigated these abnormal phenotypes in detail.

RESULTS

The orientation and morphology of the hair bundles and the positioning of the kinocilium are disturbed in aberrantly attached *Nectin-3*$^{+/-}$ HCs

There were no apparently different phenotypes in the auditory epithelium between wild-type and heterozygous *Nectin-3* (*Pvrl3*) knockout (*Nectin-3*$^{+/-}$) mice. In the *Nectin-3*$^{+/-}$ auditory epithelium, HCs were interdigitated with SCs, forming a checkerboard-like cellular pattern (Fig. 2A). The hair bundles formed a V-shape and were symmetrically arranged about the kinocilium as estimated by the immunofluorescence signals for F-actin and the basal body marker γ-tubulin, and by scanning electron microscopy (Fig. 2A,B). However, a number of HCs were aberrantly attached to each other directly, which was confirmed by transmission electron microscopy, and the orientation and morphology of the hair bundles on aberrantly attached HCs were disordered in Nectin-3-deficient (*Nectin-3*$^{-/-}$) mice in the postnatal stages (Fig. 2A-C; supplementary material Fig. S1A,B and Fig. S2).

In the *Nectin-3*$^{-/-}$ auditory epithelium, the aberrant attachments between HCs were grouped into two categories: (1) HCs attached in the same row and (2) HCs attached in different rows (Fig. 2). Aberrant attachments between HCs in the same row were more frequently observed than were aberrant attachments between HCs in different rows [64% (17, 28 and 19% from the lateral to medial attached HC pairs), versus 36% (26 and 10% for the lateral and medial HC pairs, respectively); n=4 mice]. In HCs attached in the same row, the hair bundles were orientated towards the site of attachment and asymmetrically arranged, and their morphologies were deformed (Fig. 2E,H). They were disorganised into a straight line as if they were connected (flat bundles) or split into several clumps (split bundles) (Fig. 2A; Fig. 3A,B). Flat bundles were more frequently observed than split bundles (Fig. 3C,F). The kinocilium was aberrantly located near the boundary between attached HCs (Fig. 4A,C). In HCs attached in different rows, the hair bundles were orientated towards the attached sites and asymmetrically arranged (Fig. 2F-H), and formed a straight line down the centre of HCs (Fig. 3A,B). However, the orientation and morphology of the hair bundles were less disordered in the lateral HCs (Fig. 2F,G; Fig. 3C). The kinocilium was aberrantly located near the attached sites in the medial HCs (Fig. 4A,D,E). The basal body at the base of the kinocilium was mislocalised towards the attached sites in aberrantly attached HCs (Fig. 4F). However, these abnormalities of the hair bundles and the kinocilium were not observed in unattached HCs (Figs 2, 4). These results indicate that the orientation and morphology of the hair bundles and the positioning of the kinocilium are disturbed by the aberrant attachments between *Nectin-3*$^{-/-}$ HCs.

In the vestibular epithelium of the saccule, sensory HCs and nonsensory SCs form a mosaic pattern and HCs are equipped with a uniform orientation of the hair bundles on their apical surfaces, similar to the cochlear epithelial cells (Deans et al., 2007). In contrast to the cochlear epithelium, HCs were not attached to each other and HC polarity did not change in *Nectin-3*$^{-/-}$ mice: the hair bundles face away from each other across the striola in both *Nectin-3*$^{+/-}$ and *Nectin-3*$^{-/-}$ mice (supplementary material Fig. S3B). Consistently, differential expression patterns of nectins similar to those observed in the cochlear epithelium were not observed in the surface view of the *Nectin-3*$^{+/-}$ vestibular epithelium: the immunofluorescence signals for Nectin-1, -2 and -3 were observed at the boundaries between HCs and SCs and between neighbouring SCs (supplementary material Fig. S3A). These results support the conclusion that the orientation and morphology of the hair bundles and the positioning of the kinocilium in the auditory epithelium are disturbed by the aberrant attachments between *Nectin-3*$^{-/-}$ HCs, and also support the previous conclusion (Togashi et al., 2011) that the differential expression of Nectin-1 in HCs and Nectin-3 in SCs contributes to the checkerboard-like cellular patterning in the cochlear epithelium.

The abnormal phenotypes of the hair bundles and the kinocilium are observed in aberrantly attached *Nectin-3*$^{+/-}$ HCs during development

To determine when the abnormal phenotypes of the hair bundles and the kinocilium were observed in aberrantly attached *Nectin-3*$^{-/-}$ HCs, we analysed the localisation of γ-tubulin in E16.5 mouse HCs. The maturation of the organ of Corti starts from the basal turn and proceeds to the apical turn of the cochlea; therefore, HCs in the apical turn are less mature than those in the middle turn (Lim and Anniko, 1985). In both the apical and middle turns of the *Nectin-3*$^{-/-}$ cochlea, HCs were aberrantly attached to each other

Development (2014) doi:10.1242/dev.094995

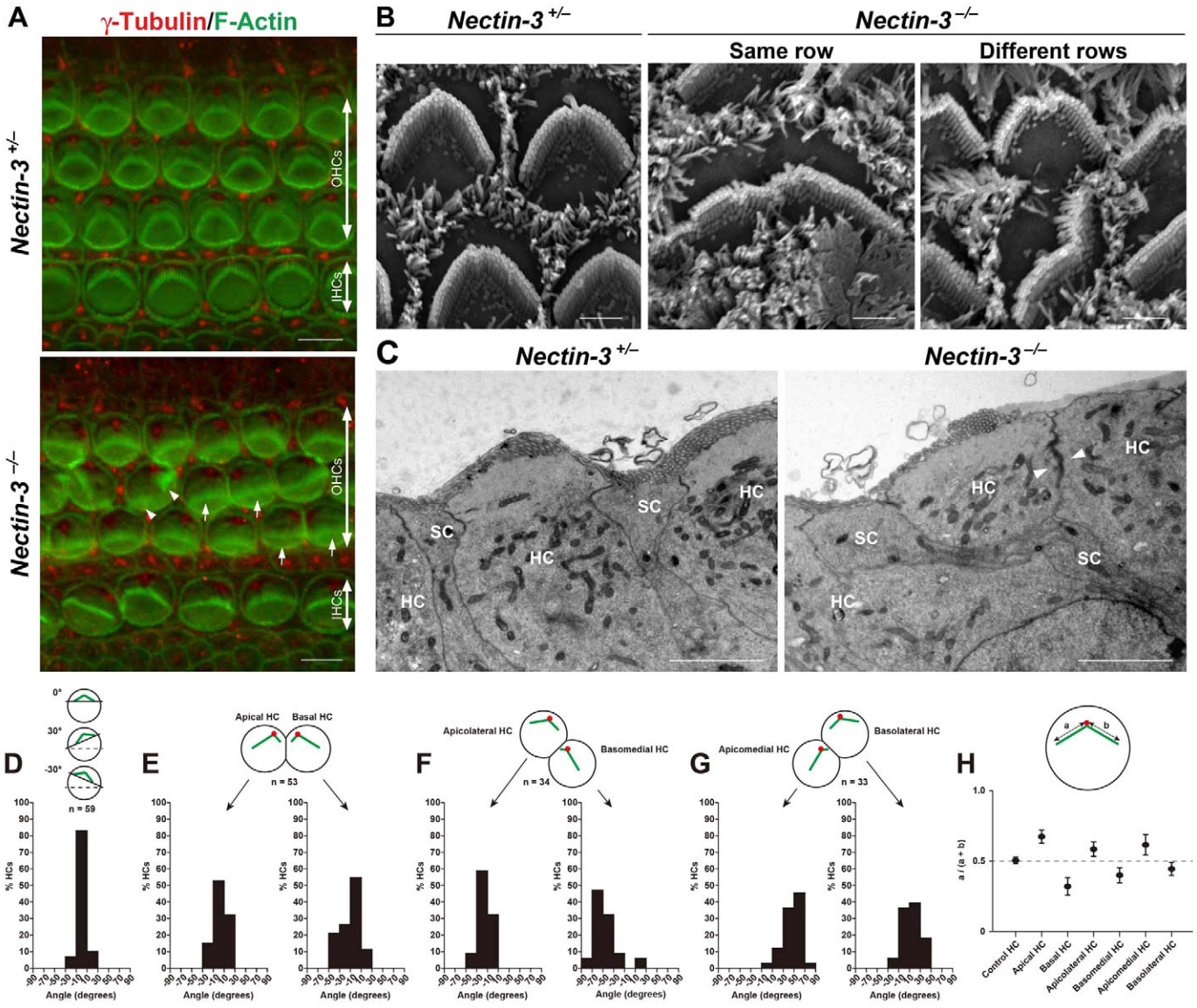

Fig. 2. Misorientation and dysmorphology of the hair bundles are observed in aberrantly attached *Nectin-3*$^{-/-}$ HCs. (A) Misorientation and dysmorphology of the hair bundles in aberrantly attached HCs in the same and different rows in *Nectin-3*$^{-/-}$ mice. F-Actin and γ-tubulin were double-stained at the basal turn of the cochlea at P1. Arrows and arrowheads indicate flat and split hair bundles, respectively. Scale bars: 5 µm. (B) Scanning electron microscopic images of HCs at P5. Scale bars: 2 µm. (C) Transmission electron microscopic images of HCs at P1. Arrowheads indicate direct attachment between HCs. HC, hair cell; SC, supporting cell. Scale bars: 2 µm. (D-H) Quantification of the orientation and symmetry of the hair bundles at the basal turn of the cochlea at P1. *Nectin-3*$^{+/-}$ mice (D), two attached HCs in the same rows in *Nectin-3*$^{-/-}$ mice (E), two attached HCs in different rows (apicolateral and basomedial HCs) in *Nectin-3*$^{-/-}$ mice (F), and two attached HCs in different rows (basolateral and apicomedial HCs) in *Nectin-3*$^{-/-}$ mice (G) are shown. The angle formed by the intersection of a line connecting two edges of the hair bundle and one parallel to the line of the inner pillar cells was measured. Clockwise and counterclockwise deviations from 0° were assigned positive and negative values, respectively. (H) Symmetry of the hair bundles (mean ± s.d.). *n*=45 [HCs in *Nectin-3*$^{+/-}$ mice (control HCs)]; *n*=30 (apical and basal HCs); *n*=22 (apicolateral and basomedial HCs); and *n*=20 (apicomedial and basolateral HCs). In schematics, red circle indicates the position of the kinocilium and green lines indicate the localisation of the hair bundles.

and the immunofluorescence signals for Nectin-1 and afadin (Mllt4 – Mouse Genome Informatics) were concentrated at the boundary between attached HCs (Fig. 5A,B). In the apical turn of the *Nectin-3*$^{+/-}$ cochlea, the signal for γ-tubulin was observed in the centre of the apical surface of HCs, whereas it was positioned at the lateral side in the middle turn (Fig. 5C; supplementary material Fig. S4A). In the *Nectin-3*$^{+/-}$ cochlea, aberrantly attached HCs were fewer than in the *Nectin-3*$^{-/-}$ cochlea and were decreased during maturation (Fig. 5B). These results indicate the correct establishment of HC polarity at E16.5, which is consistent with the previous observations that the terminal differentiation of the organ of Corti starts between E14.5 and E18.5, and that HC polarity is established by E18.5 in the mouse auditory epithelium (Kelly and Chen, 2007). By contrast, in the *Nectin-3*$^{-/-}$ cochlea at E16.5, the signal for γ-tubulin was observed in the centre of the apical surface of HCs in the apical turn even though HCs were aberrantly attached (Fig. 5C; supplementary material Fig. S4A). However, the localisation of γ-tubulin was rotated towards the attached sites in the middle turn (Fig. 5C; supplementary material Fig. S4A,B). These abnormalities were not observed in unattached HCs

Development (2014) doi:10.1242/dev.094995

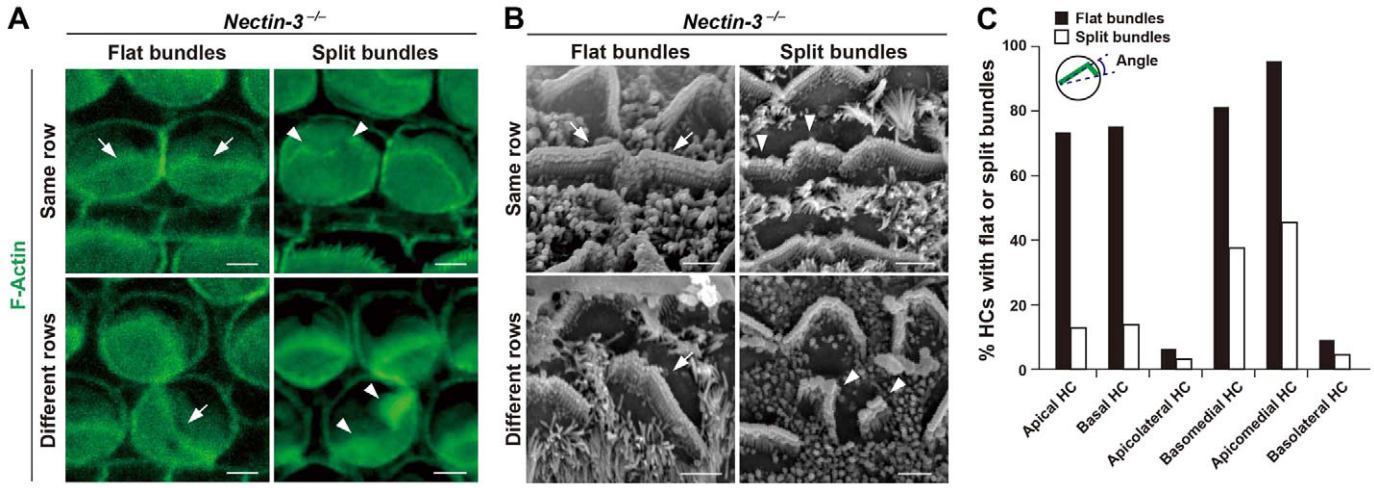

Fig. 3. Dysmorphology of the hair bundles is observed in aberrantly attached *Nectin-3*$^{-/-}$ HCs. (A,B) Dysmorphology of the hair bundles in aberrantly attached *Nectin-3*$^{-/-}$ HCs in the same and different rows at the basal turn of the cochlea at P1. Immunofluorescence microscopic images of F-actin (A) and scanning electron microscopic images (B) are shown. Arrows and arrowheads indicate flat and split bundles, respectively. A hair bundle was defined as a flat bundle when the angle between the longer side of the hair bundle and a line connecting its two edges became 30° or less. Scale bars: 2 µm. (C) Proportions of flat or split hair bundles in aberrantly attached *Nectin-3*$^{-/-}$ HCs. *n*=109 (apical and basal HCs); *n*=32 (apicolateral and basomedial HCs); and *n*=22 (apicomedial and basolateral HCs).

(Fig. 5A,C). These results indicate that the localisation of γ-tubulin is disturbed in the late stage, but not in the early stage, of the establishment of HC polarity, and suggest that the cellular machinery governing HC polarity is disturbed by the aberrant attachments between HCs during the establishment of HC polarity in the *Nectin-3*$^{-/-}$ auditory epithelium.

The localisation of the PCP components Vangl1 and Fz6 does not essentially change in aberrantly attached *Nectin-3*$^{-/-}$ HCs

Some PCP components are asymmetrically localised at the cell membranes and loss of function of PCP components causes the misorientation of the hair bundles, abnormal positioning of the

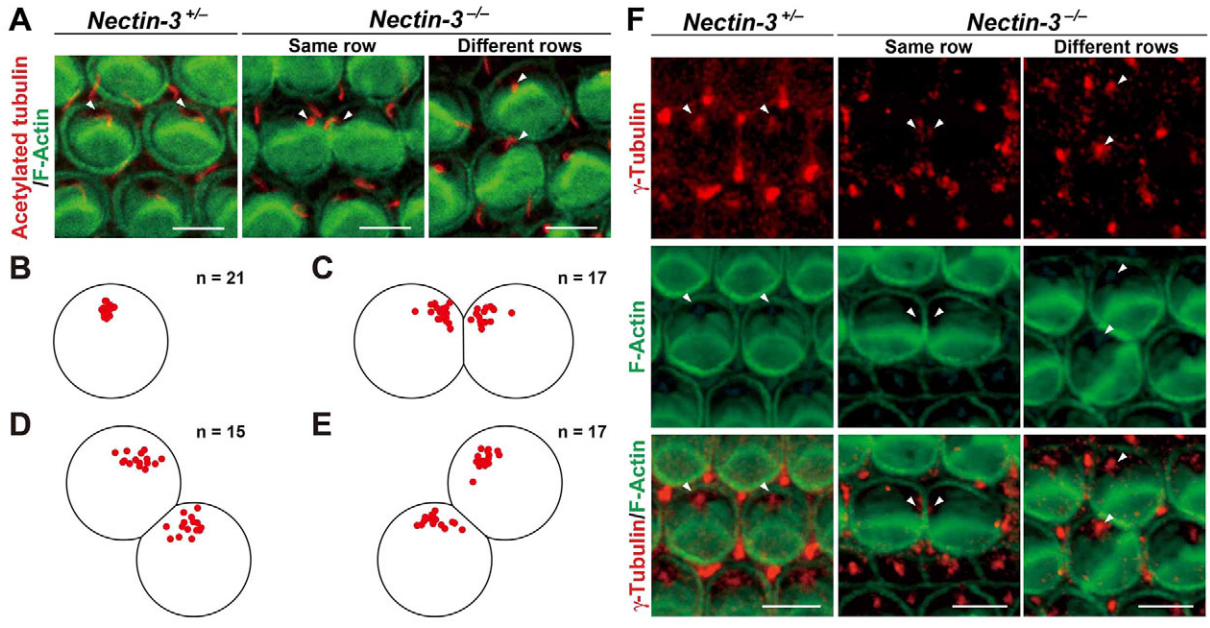

Fig. 4. Abnormal positioning of the kinocilium is observed in aberrantly attached *Nectin-3*$^{-/-}$ HCs. (A) Abnormal positioning of the kinocilium in aberrantly attached HCs in the same and different rows. F-Actin and acetylated tubulin were double-stained in the basal turn of the cochlea at P1. Arrowheads indicate the position of the kinocilium in HCs. Scale bars: 5 µm. (B-E) Summary of the position of the kinocilium. *Nectin-3*$^{+/-}$ mice (B), two attached HCs in the same rows in *Nectin-3*$^{-/-}$ mice (C), two attached HCs in different rows (apicolateral and basomedial HCs) in *Nectin-3*$^{-/-}$ mice (D), and two attached HCs in different rows (basolateral and apicomedial HCs) in *Nectin-3*$^{-/-}$ mice (E) are shown. The position of the kinocilium assessed by staining for γ-tubulin is shown in red. (F) Abnormal positioning of the basal body in aberrantly attached HCs in the same and different rows. F-Actin and γ-tubulin were double-stained in the basal turn of the cochlea at P1. Arrowheads indicate the position of the basal body in HCs. Scale bars: 5 µm.

Development (2014) doi:10.1242/dev.094995

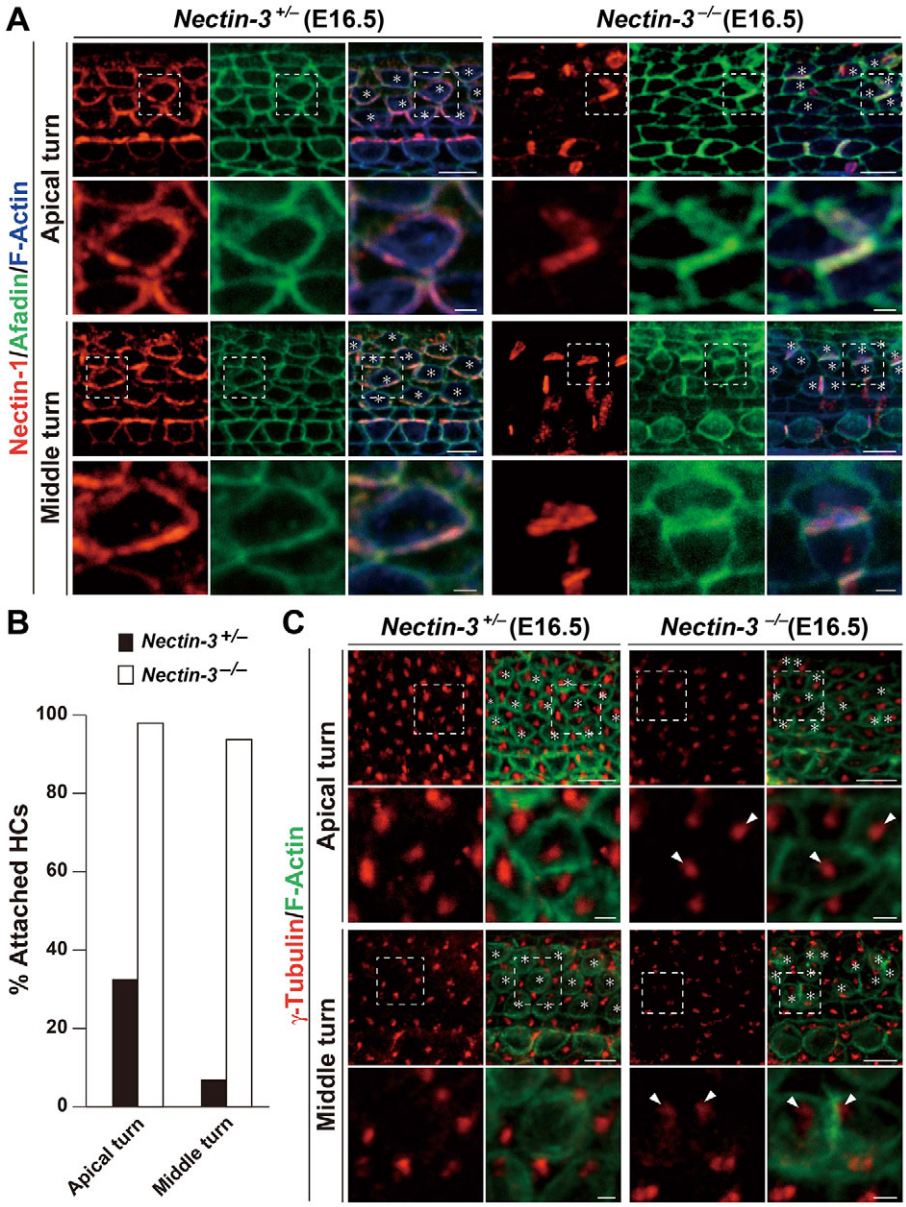

Fig. 5. Basal body is abnormally localised in aberrantly attached *Nectin-3*$^{-/-}$ HCs in the middle turn of the cochlea at E16.5. (A) Concentrations of Nectin-1 and afadin at the contact sites between aberrantly attached HCs. Nectin-1 and afadin were triple-stained with F-actin in the apical and middle turns of the cochlea at E16.5. The lower rows represent higher magnification images of the boxed areas of the upper rows. Scale bars: 5 µm (upper rows); 1 µm (lower rows). (B) Proportions of the attached HCs in the apical and middle turns of the cochlea at E16.5. The percentage of attached HCs relative to all HCs is shown. *Nectin-3*$^{+/-}$, *n*=230 (apical turn) and *n*=209 (middle turn); *Nectin-3*$^{-/-}$, *n*=193 (apical turn) and *n*=193 (middle turn). (C) Abnormal localisation of the basal body. γ-Tubulin and F-actin were double-stained in the apical and middle turns of the cochlea at E16.5. The lower rows represent higher magnification images of the boxed areas of the upper rows. Asterisks indicate HCs. The signal for γ-tubulin (arrowheads) was observed in the centre of the apical surface of HCs, even though HCs were aberrantly attached (apical turn), whereas it was rotated toward the attached site in the middle turn of the *Nectin-3*$^{-/-}$ cochlea (middle turn). Scale bars: 5 µm (upper rows); 1 µm (lower rows).

kinocilium and shortening of the cochlear duct, indicating that PCP components are implicated not only in HC polarity, but also in the cell arrangement called convergent extension (Montcouquiol et al., 2006; Wang et al., 2006a; Wang et al., 2006b). Genetic ablation of PCP components causes shortening of the cochlear duct and accumulation of HCs at the apex (Montcouquiol et al., 2003; Wang et al., 2006a). To assess convergent extension in the *Nectin-3*$^{-/-}$ cochlea, we measured the length of the cochlear duct and examined whether HCs accumulated at the apex by immunostaining for myosin VIIa. The length of the cochlear duct was not distinguishable between *Nectin-3*$^{+/-}$ and *Nectin-3*$^{-/-}$ mouse cochleae (5.58±0.23 mm versus 5.81±0.18 mm, respectively, mean ± s.d., *n*=3, *P*>0.05 by Student's *t*-test) (Fig. 6A). HCs were not accumulated at the apices of *Nectin-3*$^{+/-}$ and *Nectin-3*$^{-/-}$ mouse cochleae (Fig. 6B). To determine whether PCP components are involved in the abnormal phenotypes of the *Nectin-3*$^{-/-}$ cochlea, we compared the distributions of Vangl1 and Fz6 (Fzd6 – Mouse Genome Informatics) in *Nectin-3*$^{+/-}$ and *Nectin-3*$^{-/-}$ cochleae. In the *Nectin-3*$^{+/-}$ auditory epithelium, the immunofluorescence signals for Vangl1 and Fz6 were concentrated along the boundary between the medial edges of HCs and the lateral edges of SCs (Fig. 6C,D). The localisation of the signals for Vangl1 and Fz6 was essentially unchanged in the *Nectin-3*$^{-/-}$ auditory epithelium (Fig. 6C,D). Taken together, these results suggest that the essential function of PCP components is maintained in the *Nectin-3*$^{-/-}$ auditory epithelium.

The abnormal phenotypes of the hair bundles are also observed in aberrantly attached *Nectin-1*$^{-/-}$ HCs

Because changes in the hair bundle phenotypes of *Nectin-3*$^{-/-}$ HCs are unlikely to be related to the PCP pathway, they appear to depend on a non-autonomous effect, which probably requires Nectin-1. To verify this idea, we analysed the hair bundle phenotypes of *Nectin-1*$^{-/-}$ HCs. In *Nectin-1*$^{-/-}$ mice, HCs were aberrantly attached to each other; however, the number of these cells was much lower than that in *Nectin-3*$^{-/-}$ mice (Togashi et al., 2011). Similar to aberrantly attached *Nectin-3*$^{-/-}$ HCs, aberrantly attached *Nectin-1*$^{-/-}$ HCs also showed disturbances of the orientation and morphology of the hair bundles (supplementary material Fig. S5A), although neither

Development (2014) doi:10.1242/dev.094995

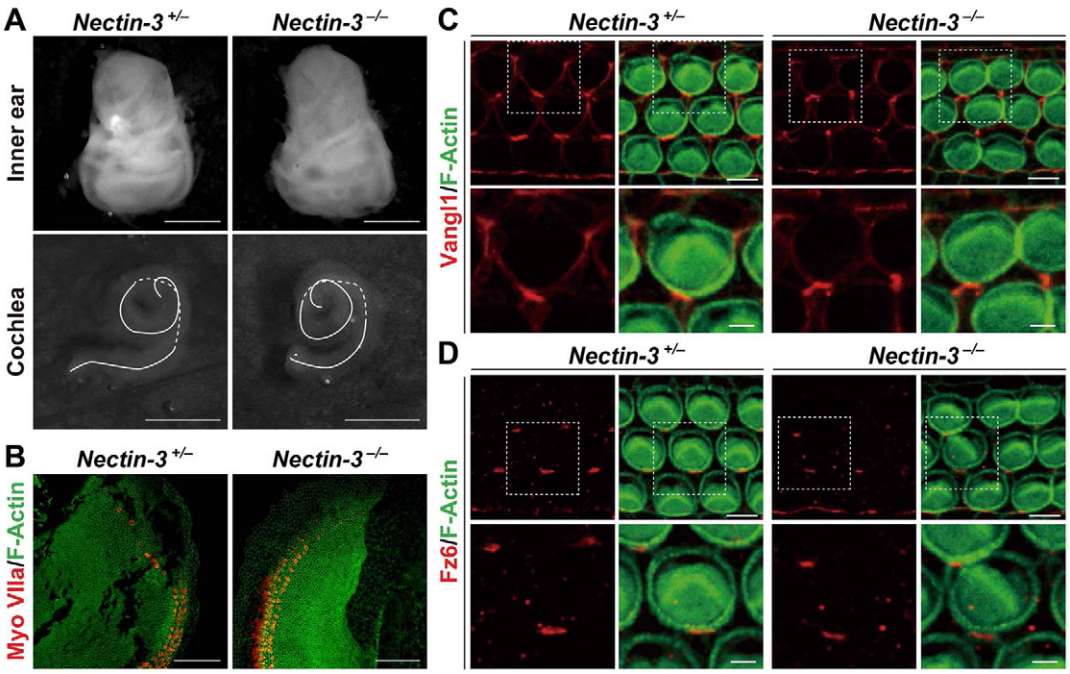

Fig. 6. Localisation of the PCP components Vangl1 and Fz6 in aberrantly attached *Nectin-3*$^{+/-}$ HCs does not change markedly. (A) General appearance of the inner ears and cochleae of *Nectin-3*$^{+/-}$ and *Nectin-3*$^{-/-}$ mice at P1. Scale bars: 1 mm. (B) Lack of accumulation of HCs at the apices of *Nectin-3*$^{+/-}$ and *Nectin-3*$^{-/-}$ cochleae. F-Actin and myosin VIIa (Myo VIIa) were double-stained in the apices of the cochlea at P1. Scale bars: 50 µm. (C,D) Double staining of Vangl1 (C) or Fz6 (D) with F-actin in the basal turn of the cochlea at P1. The lower rows represent higher magnification images of the boxed areas of the upper rows. The signals for both Vangl1 and Fz6 were concentrated along the boundary between the medial edges of HCs and the lateral edges of SCs in the *Nectin-3*$^{+/-}$ and *Nectin-3*$^{-/-}$ auditory epithelium. Scale bars: 5 µm (upper rows); 2 µm (lower rows).

Nectin-2 nor Nectin-3 was concentrated at the boundary between aberrantly attached HCs (supplementary material Fig. S5B). Thus, common abnormal phenotypes in aberrantly attached HCs strongly support the idea that the non-autonomous effect of the heterophilic interaction between Nectin-1 and -3 is essential for the correct formation of the orientation and morphology of the hair bundles.

The localisation of AJ and TJ components changes in aberrantly attached *Nectin-3*$^{+/-}$ HCs

Nectins are involved in the formation of the epithelial apical junctional complex (AJC), which includes AJs and TJs (Takai et al., 2008a; Takai et al., 2008b). We therefore assessed the distributions of components of AJs and TJs. In the surface view of the *Nectin-3*$^{+/-}$ auditory epithelium, the immunofluorescence signal for Nectin-1 was concentrated at the boundary between HCs and SCs, but not at the boundary between neighbouring SCs (Fig. 7A). Other AJ components, including Nectin-2, afadin, E-cadherin (cadherin 1 – Mouse Genome Informatics) and β-catenin, and the TJ component ZO-1 were concentrated at the boundaries between HCs and SCs and between neighbouring SCs (Fig. 7B-F). In the *Nectin-3*$^{-/-}$ auditory epithelium, the signal for Nectin-1 was markedly concentrated at the contact sites between aberrantly attached HCs, whereas it was not or was hardly observed at the boundary between HCs and SCs, presumably because Nectin-1 molecules can *trans*-interact with each other but not with Nectin-2 molecules (Fig. 7A). Furthermore, the signals for other AJ and TJ components were also markedly concentrated at the contact sites between aberrantly attached HCs, whereas they were weakly observed at the boundaries between HCs and SCs and between neighbouring SCs (Fig. 7B-F). The same results were observed irrespective of whether HCs were attached in the same or different rows.

In the lateral view of the *Nectin-3*$^{+/-}$ auditory epithelium, the signals for Nectin-1 were concentrated at the AJC area of the boundary between HCs and SCs, and those for Nectin-2, afadin and ZO-1 were concentrated at the AJC area of the boundaries between HCs and SCs and between neighbouring SCs (Fig. 7A-C,F; supplementary material Fig. S6A). However, the signals for E-cadherin and β-catenin extended further along the apicobasal axis than did those for Nectin-1, -2, afadin and ZO-1 (Fig. 7D,E; supplementary material Fig. S6A). In the *Nectin-3*$^{-/-}$ auditory epithelium, the signal for Nectin-1 was concentrated at the boundary between aberrantly attached HCs. Its distribution was extended towards the basal side and coincided with that for F-actin, whereas it was hardly observed at the boundaries between HCs and SCs and between neighbouring SCs (Fig. 7A; supplementary material Fig. S6A). The signals for other AJ and TJ components were also concentrated and their distributions were extended towards the basal side and coincided with that for F-actin at the boundary between aberrantly attached HCs, like the signal for Nectin-1, whereas they showed only weak signals at the boundaries between HCs and SCs and between neighbouring SCs (Fig. 7B-F; supplementary material Fig. S6A). The localisation of the AJ and TJ components is schematically shown in Fig. 7G. Collectively, these results indicate that the Nectin-3-mediated adhesion between HCs and SCs plays a role in the proper localisation of AJC components along the planar and apicobasal axes.

The localisation of apical-basal polarity components changes in aberrantly attached *Nectin-3*$^{+/-}$ HCs

Within the AJC, nectins are physically associated with the apicobasal polarity protein (ABP) components Patj (Inadl – Mouse Genome Informatics) and Par-3 (Pard3 – Mouse Genome

Development (2014) doi:10.1242/dev.094995

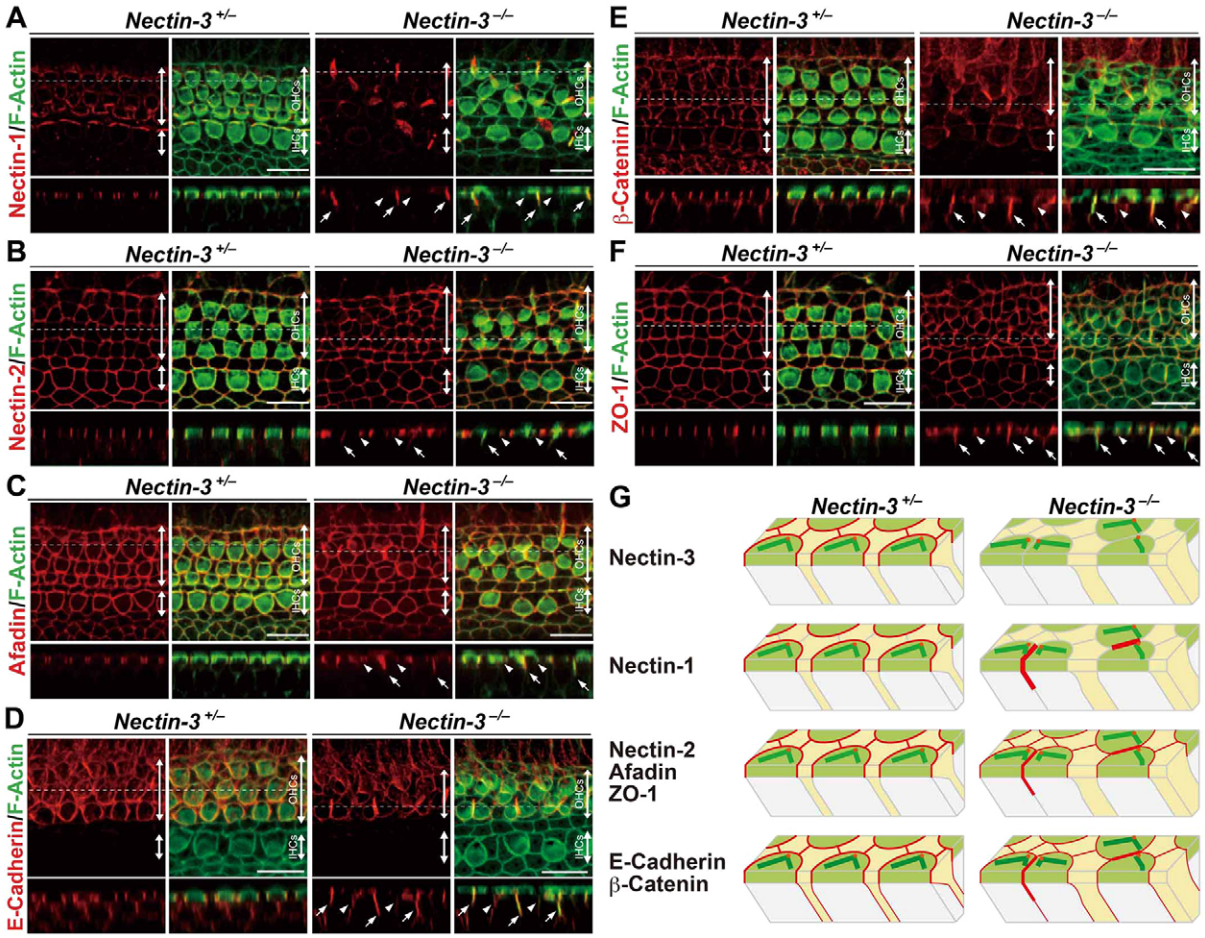

Fig. 7. Localisation of AJ and TJ components changes in aberrantly attached *Nectin-3*$^{-/-}$ HCs at P1. (A-F) Double staining of Nectin-1 (A), Nectin-2 (B), afadin (C), E-cadherin (D), β-catenin (E) and ZO-1 (F) with F-actin in the apical-middle turn of the cochlea at P1. The dashed lines in the optical *xy* sectional views correspond to the planes of the *xz* sections. Arrows indicate more concentrated and extended signals at the boundary between aberrantly attached HCs compared with those at the boundary between HCs and SCs (arrowheads). Scale bars: 10 μm. (G) Schematic of the localisation of AJ and TJ components in *Nectin-3*$^{+/-}$ and *Nectin-3*$^{-/-}$ HCs. The localisation of each AJ and TJ component is shown in red.

Informatics) (Adachi et al., 2009; Takekuni et al., 2003). We finally compared the distribution of ABP components in *Nectin-3*$^{+/-}$ and *Nectin-3*$^{-/-}$ auditory epithelia. Three major ABP complexes, namely, the apical Crumbs complex consisting of Crumbs3 (Crb3), Pals1 (Mpp5 – Mouse Genome Informatics) and Pals1-associated tight junction protein (Patj), the Par complex consisting of Par-3, Par-6 (Pard6 – Mouse Genome Informatics) and atypical protein kinase C (aPKC), and the lateral Scribble complex consisting of Scribble, discs large (Dlg1) and Lgl, are essential for epithelial ABP formation (Pieczynski and Margolis, 2011). In the surface view of the *Nectin-3*$^{+/-}$ auditory epithelium, the immunofluorescence signal for Pals1 was concentrated at the phalloidin-negative apical surface of HCs, which was polarised towards the lateral side (Fig. 8A). The signal for Par-3 was uniformly distributed along the boundaries between HCs and SCs and between neighbouring SCs (Fig. 8B). In the *Nectin-3*$^{-/-}$ auditory epithelium, the area positive for Pals1 signal was rotated towards the contact sites between aberrantly attached HCs (Fig. 8A), and the signal for Par-3 was concentrated at the contact sites between aberrantly attached HCs (Fig. 8B). These results indicate that the localisation of Pals1 and Par-3 along the planar axis changes in aberrantly attached *Nectin-3*$^{-/-}$ HCs.

In the lateral view of the *Nectin-3*$^{+/-}$ auditory epithelium, the signal for Pals1 was observed in the apical area without overlapping that for Nectin-1 at the boundary between HCs and SCs (Fig. 8A; supplementary material Fig. S6B and Fig. S7A). The signal for Par-3 was concentrated at the apical area partly overlapping that for Nectin-1 (Fig. 8B; supplementary material Fig. S6B and Fig. S7B). In the *Nectin-3*$^{-/-}$ auditory epithelium, the distribution of the signal for Pals1 was not extended towards the basal area of the boundary between aberrantly attached HCs (Fig. 8A; supplementary material Fig. S6B and Fig. S7A). The distribution of the signal for Par-3 extended into the basal area, partly overlapping that for Nectin-1 at the boundary between aberrantly attached HCs, compared with that at the boundaries between HCs and SCs and between neighbouring SCs (Fig. 8B; supplementary material Fig. S6B and Fig. S7B). These results indicate that the localisation of Par-3, but not that of Pals1, along the apicobasal axis, changes in aberrantly attached HCs. The localisation of the ABP components is schematically shown in Fig. 8C. Taken together, these results indicate that the Nectin-3-mediated adhesion between HCs and SCs is crucial for the correct localisation of Pals1 and Par-3.

DISCUSSION

We previously showed that Nectin-1 and -3 were differentially expressed in HCs and SCs, respectively, and that, in the *Nectin-3*$^{-/-}$ auditory epithelium, HCs were aberrantly attached to each other,

Development (2014) doi:10.1242/dev.094995

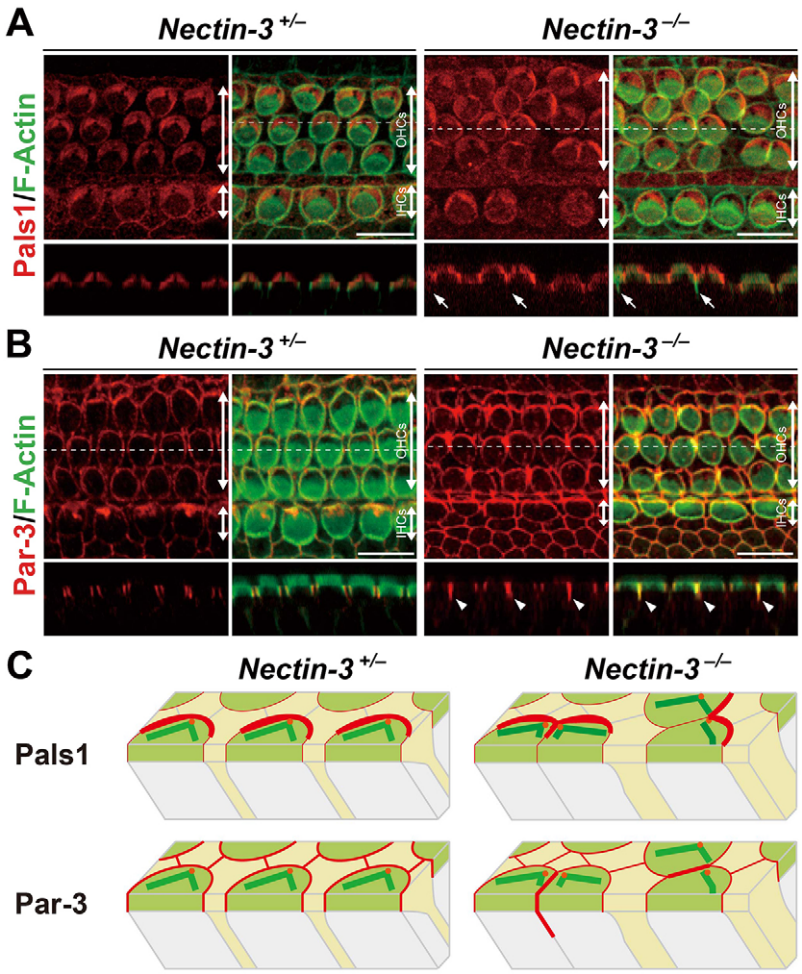

Fig. 8. Localisation of Pals1 and Par-3 changes in aberrantly attached *Nectin-3*$^{-/-}$ HCs at P1. (A,B) Double staining of Pals1 (A) or Par-3 (B) with F-actin in the apical-middle turn of the cochlea. The dashed lines in the optical *xy* sectional views in the upper rows correspond to the planes of the *xz* sections in the lower rows. Arrows indicate a lack of broad distribution of the signal for Pals1 at the boundary between aberrantly attached HCs. Arrowheads indicate the concentration and broad distribution of the signal for Par-3 at the boundary between aberrantly attached HCs. Scale bars: 10 µm. (C) Schematic of the localisation of ABP components in *Nectin-3*$^{+/-}$ and *Nectin-3*$^{-/-}$ HCs. The localisation of each ABP component is shown in red.

thereby leading to a disturbance of the checkerboard-like cellular pattern of HCs and SCs. On the basis of these observations, we proposed that the heterophilic *trans*-interaction between Nectin-1 in HCs and Nectin-3 in SCs plays a key role in the checkerboard-like cellular patterning (Togashi et al., 2011). Nectins are involved in the formation of AJs and TJs in epithelial cells (Takai et al., 2008a; Takai et al., 2008b). Here, we showed that in the *Nectin-3*$^{-/-}$ auditory epithelium, junctions between HCs and SCs were disrupted with aberrant localisation of AJ and TJ components as well as ABP components. Moreover, the absence of either Nectin-1 or -3 caused disturbances of the orientation and morphology of the hair bundles and/or the positioning of the kinocilium; however, these abnormal phenotypes were observed only in aberrantly attached HCs, but not in unattached ones. Thus, the abnormal phenotypes of HCs are likely to be due to a non-autonomous effect depending on the heterophilic interaction between Nectin-1 and -3. In addition, in *Nectin-3*$^{+/-}$ mice, the aberrant attachments between HCs were seen at E16.5, but not in the postnatal stages, suggesting that these attachments are released during maturation. However, in *Nectin-3*$^{-/-}$ mice, the abnormal phenotypes began during the migration of the hair bundles in the early developmental stages and continued until the postnatal stages. These results indicate that the changes in junction formation caused by the aberrant attachments between HCs result in the disruption of HC maturation associated with the abnormal phenotypes of the hair bundles in the *Nectin-3*$^{-/-}$ auditory epithelium.

Similar phenotypes of the hair bundles were reported in homeobox transcription factor Emx2-deficient mice and in mice mutant for the Notch ligands Dll1 and Jag2 (Holley et al., 2010; Kiernan et al., 2005). In these mice, HCs were attached to each other and lost their polarity. However, these mice showed additional abnormalities, such as defects in HC development or changes in the numbers of HCs, suggesting that the abnormal signals govern all HCs. Lack of these abnormalities suggests that Emx2 and the Notch pathway function normally in *Nectin-3*$^{-/-}$ mice.

PCP components regulate HC polarity and convergent extension (Goodrich and Strutt, 2011; Gray et al., 2011). Genetic deletion of PCP components causes hair bundle misorientation, shortening of the cochlear duct and abnormal accumulation of HCs at the apex of the duct (Montcouquiol et al., 2003; Wang et al., 2006a). Similarly, genetic deletion of ciliary proteins, such as Ift88, Kif3a and Lis1 (Pafah1b1 – Mouse Genome Informatics), causes hair bundle misorientation and shortening of the cochlear duct without affecting the asymmetric distribution of PCP components (Jones et al., 2008; Sipe et al., 2013; Sipe and Lu, 2011). In addition, there is a genetic interaction between Ift88 and Vangl2 in regulating HC polarity and convergent extension (Jones et al., 2008). By contrast, ciliary protein mutant mice, but not PCP mutant mice, show morphological changes in the hair bundles. From these findings, ciliary proteins may function either downstream of or parallel to the PCP pathway (Ezan and Montcouquiol, 2013). In *Nectin-3*$^{-/-}$ mice, the establishment of convergent extension, the localisation of Vangl1 and Fz6, and the organisation of the striolar reversal zone in the vestibular epithelium were all normal; however, the orientation and morphology of the hair bundles were disrupted only in aberrantly

Development (2014) doi:10.1242/dev.094995

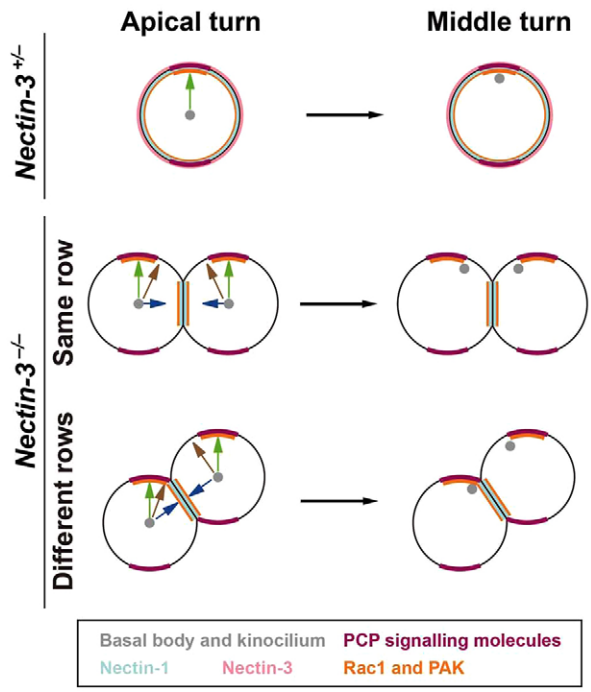

Fig. 9. Model of the abnormal positioning of the basal body and the kinocilium in aberrantly attached *Nectin-3*$^{-/-}$ HCs. The details are described in the Discussion.

attached HCs. These results suggest that PCP components do not significantly contribute to the abnormal phenotypes of *Nectin-3*$^{-/-}$ HCs, but rather that some signal(s) initiated from ciliary proteins is altered by the abnormal attachments in *Nectin-3*$^{-/-}$ HCs.

How are the signals regulating HC polarity disturbed by the aberrant attachments between HCs? Are there some common downstream signals between PCP components and ciliary proteins? One of the candidates for a common signalling pathway is the Rac1/p21-activated kinase (PAK) signalling pathway. This signalling pathway serves as an effector of the Wnt pathway in PCP (Habas et al., 2003) and ciliary proteins (Sipe et al., 2013; Sipe and Lu, 2011), and the *trans*-interactions of nectins induce the activation of Rac1 (Kawakatsu et al., 2002). In Madin–Darby canine kidney cells, Rac1 is transiently activated by nectins during the initiation of their *trans*-interactions and then inactivated once the *trans*-interactions are established (Kitt and Nelson, 2011). Rac1/PAK signalling regulates the organisation of the actin and microtubule cytoskeletons (Bokoch, 2003), and *Rac1* knockout mice showed defects in HC morphogenesis similar to those observed in *Nectin-3*$^{-/-}$ HCs (Grimsley-Myers et al., 2009). To evaluate the mechanism underlying HC polarity, we attempted to examine the activation of Rac1/PAK signalling in the *Nectin-3*$^{-/-}$ auditory epithelium, but were unable to determine whether this pathway was activated (data not shown). Therefore, it remains to be elucidated whether Rac1 is activated only at crucial areas of HCs and in the crucial stages of development of the auditory epithelium when the orientation and morphology of the hair bundles and the positioning of the kinocilium are determined, although it can be speculated that the misorientation and dysmorphology of the hair bundles in the *Nectin-3*$^{-/-}$ auditory epithelium may be caused by the ectopic activation of Rac1/PAK signalling.

The ABP component Patj binds to nectins (Adachi et al., 2009) and forms a ternary complex with Pals1 and Crb3 (Makarova et al., 2003). This ternary complex is upstream of the apical ABP complex Par-3–Par-6–aPKC in epithelial cells (Hurd et al., 2003). Par-3 binds to nectins and regulates the formation of TJs cooperatively with afadin in epithelial cells (Ooshio et al., 2007; Takekuni et al., 2003). The ABP component Scribble is genetically associated with Vangl (Montcouquiol et al., 2003). However, the molecular links between AJC and PCP components remain unclear. Here, we showed that Pals1 and Par-3 were aberrantly localised in aberrantly attached *Nectin-3*$^{-/-}$ HCs and that AJC formation was disturbed at the boundary between aberrantly attached HCs. At the boundary between aberrantly attached HCs, the distributions of the AJC components Nectin-1, Nectin-2, afadin, E-cadherin, β-catenin and ZO-1, and the ABP component Par-3, all of which were concentrated there, extended along the apicobasal axis. Pals1 localised to the apical surface of HCs was rotated towards the attached sites. Par-3 regulates microtubule dynamics and centrosome orientation through dynein (Schmoranzer et al., 2009) and the cadherin–catenin complex regulates microtubule dynamics (Harris and Tepass, 2010). Together with these previous findings, it can be speculated that the homophilic interaction of Nectin-1 at the boundary between aberrantly attached *Nectin-3*$^{-/-}$ HCs alters microtubule dynamics through positional changes in AJC and ABP components. This is consistent with the previous findings that genetic deletion of microtubule-associated ciliary proteins such as Ift88, Kif3a and Lis1 resulted in a disruption of HC polarity and morphological changes in the hair bundles (Sipe et al., 2013; Sipe and Lu, 2011). Therefore, heterophilic interaction of nectins probably leads to an elaborate checkerboard-like cellular pattern by arranging the localisation of AJC and ABP components and by controlling microtubule dynamics and, thus, contributing to the formation of HC polarity and the morphology of the hair bundles.

The detailed molecular mechanisms underlying the orientation and morphology of the hair bundles, the positioning of the kinocilium and the localisation of PCP components remain unknown, but we propose here a model for the abnormal positioning of the basal body and the kinocilium in aberrantly attached *Nectin-3*$^{-/-}$ HCs, as schematically shown in Fig. 9. In the *Nectin-3*$^{+/-}$ auditory epithelium, the PCP pathway is activated along the medial-lateral side axis by extracellular cues from PCP signalling during the maturation of the cochlea. Because Nectin-1 and -3 are uniformly distributed along the boundary between HCs and SCs, signals such as Rac1 and PAK should be appropriately activated at the lateral edge to propagate the PCP pathway. As a result, the basal body and the kinocilium (grey dot) move towards the lateral side of HCs (green arrows). In the *Nectin-3*$^{-/-}$ auditory epithelium, however, at the contact sites between aberrantly attached HCs, Nectin-1 accumulates presumably because Nectin-1 molecules can *trans*-interact with each other but not with Nectin-2, and the signals may be activated by the Nectin-1–afadin complex; therefore, the basal body and the kinocilium move towards the sum (brown arrows) of the signals induced by the extracellular cues of PCP signalling (green arrows) and the signals induced by aberrant attachments between HCs (blue arrows), thus causing the aberrant positioning of the basal body and the kinocilium and the subsequent misorientation and dysmorphology of the hair bundles. If this is the case, these mechanisms may provide insights into why HCs are interdigitated with SCs to form a checkerboard-like cellular pattern in the auditory epithelium. The separation of HCs by SCs, which leads to the checkerboard-like cellular patterning of these two types of cells, is at least required for HC polarity.

Development (2014) doi:10.1242/dev.094995

MATERIALS AND METHODS

Mice

Nectin-1 (*Pvrl1*) knockout (*Nectin-1*$^{-/-}$) and *Nectin-3* (*Pvrl3*) knockout (*Nectin-3*$^{+/-}$ and *Nectin-3*$^{-/-}$) mice were generated as described (Inagaki et al., 2005). The animal experiments were approved by the Institutional Animal Care and Use Committee and carried out according to the Kobe University Animal Experimental Regulations.

Antibodies

The following antibodies (Abs) were used: mouse anti-acetylated tubulin monoclonal Ab (mAb) (T6793, 1:500, Sigma-Aldrich); rat anti-mouse Nectin-1 mAb (D146-3, 1:200, MBL); rat anti-mouse Nectin-2 mAb (D083-3, 1:200, MBL); rabbit anti-l-afadin polyclonal Ab (pAb) (A0349, 1:200, Sigma-Aldrich); rabbit anti-γ-tubulin pAb (T3195, 1:200, Sigma-Aldrich); rabbit anti-myosin VIIa pAb (25-6790, 1:400, Proteus BioSciences); rabbit anti-Vangl1 mAb (HPA025235, 1:2000, Sigma-Aldrich); mouse anti-Fz6 mAb (1:5000, a gift from Dr J. Nathans, Johns Hopkins University, MD, USA); rat anti-E-cadherin mAb (1:500, a gift from Dr M. Takeichi, RIKEN, Kobe, Japan); mouse anti-β-catenin mAb (1:400, a gift from Dr M. J. Wheelock, University of Nebraska, NE, USA); mouse anti-ZO-1 mAb (339100, 1:100, Invitrogen); rabbit anti-protein associated with Lin-7 (Pals1) pAb (sc-33831, 1:100, Santa Cruz Biotechnology); and rabbit anti-Par-3 pAb (07-330, 1:400, Millipore). The primary Abs were visualised using donkey fluorochrome-conjugated secondary Abs (1:400). The fluorochromes used were Cy3 and Cy5 (Millipore). F-Actin was visualised using Alexa 488-conjugated phalloidin (1:100, Invitrogen).

Immunofluorescence microscopy

For whole-mount immunofluorescence microscopy, dissected organs were fixed with 2% paraformaldehyde (PFA) in Hanks' balanced salt solution at room temperature (RT) for 30 minutes, washed in PBS, and then permeabilised with 0.2% Triton X-100 in PBS for 15 minutes. The samples were blocked with a blocking solution containing 10% normal donkey serum and 1% bovine serum albumin in PBS at RT for 30 minutes, followed by incubation with primary Abs in the blocking solution at 4°C overnight. The samples were washed with PBS, then incubated in secondary Abs in Can Get Signal Solution A (Toyobo Life Science) at RT for 75 minutes. The samples were flat-mounted on glass slides with glycerol gelatine (Sigma-Aldrich). A *z*-stack of whole-mount cochleae was imaged using a confocal microscope (LSM700; Carl Zeiss). Fluorescence intensity was measured using ImageJ software (NIH).

Scanning electron microscopy

Mouse cochlear samples were fixed with 2.5% glutaraldehyde (GA) and 2% PFA in 0.1 M phosphate buffer (PB) at RT for 30 minutes, and then prepared using the osmium-thiocarbohydrazide-osmium-thiocarbohydrazide-osmium method as previously described (Hunter-Duvar, 1978). The samples were viewed by scanning electron microscopy.

Transmission electron microscopy

Mouse cochlear samples were fixed with 2.5% GA and 2% PFA in 0.1 M PB at RT for 1 hour. They were washed in PBS, transferred to a 25% sucrose solution, then embedded in OCT compound and frozen on dry ice. The samples were viewed with transmission electron microscopy.

Quantitative assessment of the orientation of the hair bundles

For quantification of the orientation of the hair bundles, HCs at the basal turns of *Nectin-3*$^{-/-}$ and littermate control cochleae were analysed at P1. To evaluate the angle of the orientation of the hair bundles, the angle formed by the intersection of a line connecting the free ends of the stereocilia and a line parallel to the pillar cells was measured using ImageJ software.

Acknowledgements

We thank Drs J. Nathans (Johns Hopkins University), M. Takeichi (RIKEN) and M. J. Wheelock (University of Nebraska) for the generous gifts of reagents; Drs T. Uemura (Kyoto University) and M. Furuse (Kobe University) for helpful discussions and critical reading of the manuscript; Dr H. Sakaguchi (Kyoto Prefectural University of Medicine) for performing the osmium-thiocarbohydrazide-osmium-thiocarbohydrazide-osmium method; and Dr S. Kitajiri (Kyoto University) for analysis of the vestibular system.

Competing interests

The authors declare no competing financial interests.

Author contributions

T.F., K.K., S.W., H.T. and A.M. designed and performed experiments, analysed results, and helped write the paper. K.H. designed experiments and analysed results. Y.R. and Y.T. designed experiments, analysed results and wrote the paper.

Funding

This work was supported by the Global Centers of Excellence Programs; the Targeted Proteins Research Program from the Ministry of Education, Culture, Sports, Science and Technology in Japan; Grants-in-Aid from the Japan Society for the Promotion of Science; and the Core Research for Evolutional Science and Technology from the Japanese Science and Technology Agency. K. Kominami is a recipient of a Research Fellowship from the Japan Society for the Promotion of Science for Young Scientists (DC1).

Supplementary material

Supplementary material available online at
http://dev.biologists.org/lookup/suppl/doi:10.1242/dev.094995/-/DC1

References

Adachi, M., Hamazaki, Y., Kobayashi, Y., Itoh, M., Tsukita, S., Furuse, M. and Tsukita, S. (2009). Similar and distinct properties of MUPP1 and Patj, two homologous PDZ domain-containing tight-junction proteins. *Mol. Cell. Biol.* **29**, 2372-2389.

Barald, K. F. and Kelley, M. W. (2004). From placode to polarization: new tunes in inner ear development. *Development* **131**, 4119-4130.

Bokoch, G. M. (2003). Biology of the p21-activated kinases. *Annu. Rev. Biochem.* **72**, 743-781.

Deans, M. R., Antic, D., Suyama, K., Scott, M. P., Axelrod, J. D. and Goodrich, L. V. (2007). Asymmetric distribution of prickle-like 2 reveals an early underlying polarization of vestibular sensory epithelia in the inner ear. *J. Neurosci.* **27**, 3139-3147.

Denman-Johnson, K. and Forge, A. (1999). Establishment of hair bundle polarity and orientation in the developing vestibular system of the mouse. *J. Neurocytol.* **28**, 821-835.

Ezan, J. and Montcouquiol, M. (2013). Revisiting planar cell polarity in the inner ear. *Semin. Cell Dev. Biol.* **24**, 499-506.

Goodrich, L. V. and Strutt, D. (2011). Principles of planar polarity in animal development. *Development* **138**, 1877-1892.

Gray, R. S., Roszko, I. and Solnica-Krezel, L. (2011). Planar cell polarity: coordinating morphogenetic cell behaviors with embryonic polarity. *Dev. Cell* **21**, 120-133.

Grimsley-Myers, C. M., Sipe, C. W., Géléoc, G. S. and Lu, X. (2009). The small GTPase Rac1 regulates auditory hair cell morphogenesis. *J. Neurosci.* **29**, 15859-15869.

Habas, R., Dawid, I. B. and He, X. (2003). Coactivation of Rac and Rho by Wnt/Frizzled signaling is required for vertebrate gastrulation. *Genes Dev.* **17**, 295-309.

Harris, T. J. and Tepass, U. (2010). Adherens junctions: from molecules to morphogenesis. *Nat. Rev. Mol. Cell Biol.* **11**, 502-514.

Harrison, O. J., Vendome, J., Brasch, J., Jin, X., Hong, S., Katsamba, P. S., Ahlsen, G., Troyanovsky, R. B., Troyanovsky, S. M., Honig, B. et al. (2012). Nectin ectodomain structures reveal a canonical adhesive interface. *Nat. Struct. Mol. Biol.* **19**, 906-915.

Holley, M., Rhodes, C., Kneebone, A., Herde, M. K., Fleming, M. and Steel, K. P. (2010). Emx2 and early hair cell development in the mouse inner ear. *Dev. Biol.* **340**, 547-556.

Hunter-Duvar, I. M. (1978). A technique for preparation of cochlear specimens for assessment with the scanning electron microscope. *Acta Otolaryngol.* **85 Suppl.** S3-S23.

Hurd, T. W., Gao, L., Roh, M. H., Macara, I. G. and Margolis, B. (2003). Direct interaction of two polarity complexes implicated in epithelial tight junction assembly. *Nat. Cell Biol.* **5**, 137-142.

Ikeda, W., Kakunaga, S., Itoh, S., Shingai, T., Takekuni, K., Satoh, K., Inoue, Y., Hamaguchi, A., Morimoto, K., Takeuchi, M. et al. (2003). Tage4/Nectin-like molecule-5 heterophilically trans-interacts with cell adhesion molecule Nectin-3 and enhances cell migration. *J. Biol. Chem.* **278**, 28167-28172.

Inagaki, M., Irie, K., Ishizaki, H., Tanaka-Okamoto, M., Morimoto, K., Inoue, E., Ohtsuka, T., Miyoshi, J. and Takai, Y. (2005). Roles of cell-adhesion molecules nectin 1 and nectin 3 in ciliary body development. *Development* **132**, 1525-1537.

Jones, C., Roper, V. C., Foucher, I., Qian, D., Banizs, B., Petit, C., Yoder, B. K. and Chen, P. (2008). Ciliary proteins link basal body polarization to planar cell polarity regulation. *Nat. Genet.* **40**, 69-77.

Kawakatsu, T., Shimizu, K., Honda, T., Fukuhara, T., Hoshino, T. and Takai, Y. (2002). Trans-interactions of nectins induce formation of filopodia and Lamellipodia through the respective activation of Cdc42 and Rac small G proteins. *J. Biol. Chem.* **277**, 50749-50755.

Kelly, M. and Chen, P. (2007). Shaping the mammalian auditory sensory organ by the planar cell polarity pathway. *Int. J. Dev. Biol.* **51**, 535-547.

Kiernan, A. E., Cordes, R., Kopan, R., Gossler, A. and Gridley, T. (2005). The Notch ligands DLL1 and JAG2 act synergistically to regulate hair cell development in the mammalian inner ear. *Development* **132**, 4353-4362.
Kitt, K. N. and Nelson, W. J. (2011). Rapid suppression of activated Rac1 by cadherins and nectins during de novo cell-cell adhesion. *PLoS ONE* **6**, e17841.
Klein, T. J. and Mlodzik, M. (2005). Planar cell polarization: an emerging model points in the right direction. *Annu. Rev. Cell Dev. Biol.* **21**, 155-176.
Lim, D. J. and Anniko, M. (1985). Developmental morphology of the mouse inner ear. A scanning electron microscopic observation. *Acta Otolaryngol. Suppl.* **422**, 1-69.
Makarova, O., Roh, M. H., Liu, C. J., Laurinec, S. and Margolis, B. (2003). Mammalian Crumbs3 is a small transmembrane protein linked to protein associated with Lin-7 (Pals1). *Gene* **302**, 21-29.
Montcouquiol, M., Rachel, R. A., Lanford, P. J., Copeland, N. G., Jenkins, N. A. and Kelley, M. W. (2003). Identification of Vangl2 and Scrb1 as planar polarity genes in mammals. *Nature* **423**, 173-177.
Montcouquiol, M., Sans, N., Huss, D., Kach, J., Dickman, J. D., Forge, A., Rachel, R. A., Copeland, N. G., Jenkins, N. A., Bogani, D. et al. (2006). Asymmetric localization of Vangl2 and Fz3 indicate novel mechanisms for planar cell polarity in mammals. *J. Neurosci.* **26**, 5265-5275.
Ooshio, T., Fujita, N., Yamada, A., Sato, T., Kitagawa, Y., Okamoto, R., Nakata, S., Miki, A., Irie, K. and Takai, Y. (2007). Cooperative roles of Par-3 and afadin in the formation of adherens and tight junctions. *J. Cell Sci.* **120**, 2352-2365.
Pieczynski, J. and Margolis, B. (2011). Protein complexes that control renal epithelial polarity. *Am. J. Physiol.* **300**, F589-F601.
Schmoranzer, J., Fawcett, J. P., Segura, M., Tan, S., Vallee, R. B., Pawson, T. and Gundersen, G. G. (2009). Par3 and dynein associate to regulate local microtubule dynamics and centrosome orientation during migration. *Curr. Biol.* **19**, 1065-1074.
Sipe, C. W. and Lu, X. (2011). Kif3a regulates planar polarization of auditory hair cells through both ciliary and non-ciliary mechanisms. *Development* **138**, 3441-3449.
Sipe, C. W., Liu, L., Lee, J., Grimsley-Myers, C. and Lu, X. (2013). Lis1 mediates planar polarity of auditory hair cells through regulation of microtubule organization. *Development* **140**, 1785-1795.
Takai, Y., Ikeda, W., Ogita, H. and Rikitake, Y. (2008a). The immunoglobulin-like cell adhesion molecule nectin and its associated protein afadin. *Annu. Rev. Cell Dev. Biol.* **24**, 309-342.
Takai, Y., Miyoshi, J., Ikeda, W. and Ogita, H. (2008b). Nectins and nectin-like molecules: roles in contact inhibition of cell movement and proliferation. *Nat. Rev. Mol. Cell Biol.* **9**, 603-615.
Takekuni, K., Ikeda, W., Fujito, T., Morimoto, K., Takeuchi, M., Monden, M. and Takai, Y. (2003). Direct binding of cell polarity protein PAR-3 to cell-cell adhesion molecule nectin at neuroepithelial cells of developing mouse. *J. Biol. Chem.* **278**, 5497-5500.
Togashi, H., Kominami, K., Waseda, M., Komura, H., Miyoshi, J., Takeichi, M. and Takai, Y. (2011). Nectins establish a checkerboard-like cellular pattern in the auditory epithelium. *Science* **333**, 1144-1147.
Wang, J., Hamblet, N. S., Mark, S., Dickinson, M. E., Brinkman, B. C., Segil, N., Fraser, S. E., Chen, P., Wallingford, J. B. and Wynshaw-Boris, A. (2006a). Dishevelled genes mediate a conserved mammalian PCP pathway to regulate convergent extension during neurulation. *Development* **133**, 1767-1778.
Wang, Y., Guo, N. and Nathans, J. (2006b). The role of Frizzled3 and Frizzled6 in neural tube closure and in the planar polarity of inner-ear sensory hair cells. *J. Neurosci.* **26**, 2147-2156.
Yoshida, N. and Liberman, M. C. (1999). Stereociliary anomaly in the guinea pig: effects of hair bundle rotation on cochlear sensitivity. *Hear. Res.* **131**, 29-38.